Wireless and passive temperature indicator utilizing the large hysteresis of magnetic shape memory alloys

Bernhard Bergmair, Jian Liu, Thomas Huber, Oliver Gutfleisch, and Dieter Suess

Citation: Applied Physics Letters **101**, 042412 (2012); doi: 10.1063/1.4739836
View online: http://dx.doi.org/10.1063/1.4739836
View Table of Contents: http://scitation.aip.org/content/aip/journal/apl/101/4?ver=pdfcov
Published by the AIP Publishing

Wireless and passive temperature indicator utilizing the large hysteresis of magnetic shape memory alloys

Bernhard Bergmair,[1,2,a)] Jian Liu,[3] Thomas Huber,[1,2] Oliver Gutfleisch,[4] and Dieter Suess[1,5]
[1]*Institute of Solid State Physics, Vienna University of Technology, Wiedner Hauptstr. 8, 1040 Wien, Austria*
[2]*Institute of Analysis and Scientific Computing, Vienna University of Technology, Wiedner Hauptstr. 8, 1040 Wien, Austria*
[3]*IFW Dresden, Institute for Metallic Materials, P.O. Box 270116, D-01171 Dresden, Germany*
[4]*Department of Materials Science, Technische Universität Darmstadt, 64287 Darmstadt, Germany*
[5]*SuessCo KG, Rathausplatz 18, 3130 Herzogenburg, Austria*

(Received 22 May 2012; accepted 16 July 2012; published online 26 July 2012)

An ultra-low cost, wireless magnetoelastic temperature indicator is presented. It comprises a magnetostrictive amorphous ribbon, a Ni-Mn-Sn-Co magnetic shape memory alloy with a highly tunable transformation temperature, and a bias magnet. It allows to remotely detect irreversible changes due to transgressions of upper or lower temperature thresholds. Therefore, the proposed temperature indicator is particularly suitable for monitoring the temperature-controlled supply chain of, e.g., deep frozen and chilled food or pharmaceuticals. © *2012 American Institute of Physics*. [http://dx.doi.org/10.1063/1.4739836]

The presented temperature indicator is based on the technology of magnetoelastic resonance sensors. These sensors are used millionfold in their simplest form in electronic article surveillance (EAS).[1] In recent years, there has been an increasing interest in magnetoelastic resonance sensors, as they provide an opportunity to remotely monitor a variety of quantities. The sensors are passive and material costs are so low that it is possible to use them on a disposable basis. They are applicable for measuring temperature, fluid flow velocity and density, strain, pressure and mass, humidity, *p*H, concentration of ammonia, glucose, carbon dioxide, *Escherichia coli*, sludge accumulation within biliary stents etc.[2–5]

The aimed application for the presented temperature indicator is monitoring the supply chain of temperature-sensitive products like chilled and deep-frozen food or pharmaceuticals. The sensors just have to be attached to the products before shipment. At delivery, the sensors inside the cargo are checked remotely by just moving the cargo by a magnetic antenna. The antenna will give alarm if any of the products have experienced a transgression of the according temperature threshold.

In this Letter, we present a magnetoelastic resonance temperature indicator, which is able to remember such transgressions of upper or lower temperature thresholds.

The basic sensing element of magnetoelastic resonance sensors is a low-cost amorphous ferromagnetic magnetostrictive ribbon ("resonator"). As a consequence of the magnetoelastic effect, mechanical vibrations of the resonator can be generated remotely by applying a time varying magnetic field. After turning off this excitation field, the resonator oscillates freely at its resonant frequency for some milliseconds. It thereby produces a time varying magnetic moment (inverse magnetoelastic or Villari effect[6]), which can be detected remotely again.

The resonant frequency of the resonator's longitudinal oscillation mode is given by[7]

$$f = \frac{1}{2L}\sqrt{\frac{E}{\rho(1-\nu)}}, \tag{1}$$

where L is the resonator length, E is the resonator's Young's Modulus, ρ its mass density, and ν its Poisson ratio. For a magnetostrictive material, Young's modulus is not a constant. Due to the Delta-E-effect, it is coupled to the magnetic properties of the materials and hence changes if a magnetic field H is applied.[8,9]

$$\frac{1}{E(H)} = \frac{1}{E_s} + 9\,\frac{\lambda_s^2\,\mu_0}{J_s^2}\;\chi(H)\,m(H)^2. \tag{2}$$

E_s is Young's modulus at saturation magnetization, λ_s the saturation magnetostriction, μ_0 the magnetic constant, χ the differential susceptibility, J_s the magnetic saturation polarization, and m is the relative magnetization in parallel to the resonator's long axis. The magnetization of the resonator constitutes its operating point as the magnetization not only determines the resonator's resonant frequency but also its response to external AC fields and hence the sensors signal strength.[10] The magnetization is obtained by a constant magnetic field ("bias field") which can be generated by a magnetic coil or a permanent magnet ("bias magnet"), respectively.

For the presented temperature indicator, this concept was enhanced by adding a so called "switch." The switch is made from a magnetic shape memory alloy (MSMA), which irreversibly shifts the operating point when the temperature transgresses certain temperature limits due to a first order phase transition.[11] Figure 1 shows the used sensor design. The MSMA switch is placed in parallel to the bias magnet and the resonator (without touching it). Depending on its temperature history, the MSMA can either be in its

a)Electronic mail: bernhard.bergmair@tuwien.ac.at.

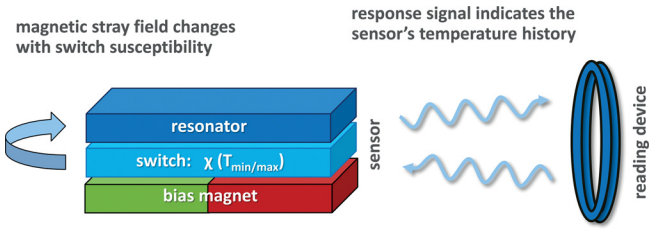

FIG. 1. Working principle of a magnetoelastic resonance temperature indicator comprising a magnetostrictive amorphous alloy (resonator), a permanent magnet (bias magnet), and an integrated MSMA element (switch) for monitoring lower or upper temperature thresholds.

paramagnetic martensite state with low susceptibility or in its ferromagnetic austenite state with high susceptibility. According to the actual susceptibility, the switch gets more or less magnetized by the stray field of the bias magnet. The stray field of the switch on its part alters the total magnetic field the resonator is exposed to, thus, shifting the resonator's resonant frequency (see Figure 2). This means that the sensor's resonant frequency indicates the state of the switch and hence its temperature history.

A related principle was used by Nakamura *et al.*[12] They used a low Curie temperature material for the switch to obtain a temperature sensor, which is very sensitive near the Curie temperature of the switch. However, the susceptibility change due to variations of the temperature is highly reversible for this second order phase transition as it shows no thermal hysteresis. Hence, the susceptibility of the switch always depends on its actual temperature, not on its temperature history. Thus, low Curie temperature materials are a good choice for sensors measuring the actual temperature. A temperature indicator, on the contrary, should indicate if certain temperature limits have at least once been transgressed—independent from the actual temperature. Therefore, a switch material with a distinct thermal hysteresis is required.

We, therefore, chose the MSMA Ni-Mn-Sn-Co as switch material. MSMAs have gained lots of interests as they could be used as ferromagnetic actuators[13–15] or in magnetocaloric applications.[16–20] The metamagnetic shape memory alloys Ni-Mn-Sn-Co exists in its paramagnetic martensite state at low temperature and in its ferromagnetic austenite state at high temperature. The phase transition is of first order and, therefore, shows a distinct thermal hysteresis. This means that the transition is partially irreversible in the range of the thermal hysteresis. If the initially martensitic switch once exceeds a certain upper temperature threshold (upper transition temperature), it will remain in the austenite state even if the temperature drops below the upper transition temperature again. It, therefore, remembers the transgression. Only if the temperature comes below the lower transition temperature, the MSMA switches back to the martensite state, whereby the information of the initial transgression is deleted. The principle works vice versa for lower temperature thresholds.

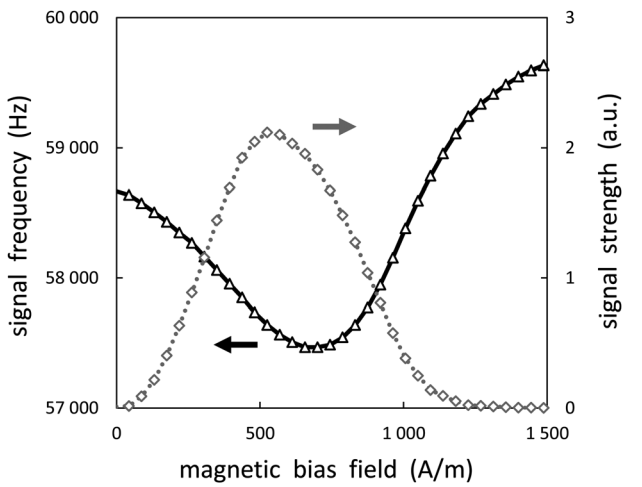

FIG. 2. Resonant frequency (continuous line) and signal amplitude (dashed line) of two adjacent magnetostrictive amorphous ribbons (38 mm × 12.5 mm) taken from a sensormatic EAS hard tag plotted against the strength of a longitudinally applied homogeneous magnetic bias field.

The Ni-Mn-Sn-Co system was previously reported in the bulk form,[21] which exhibited a thermal hysteresis of about 10 K, which is too small to fulfill the demand of irreversibility in practice. Within this work, special Ni-Mn-Sn-Co alloys were developed to meet following requirements: (i) a high accuracy of the lower/upper temperature threshold, which demands a sharp magnetostructural transition; (ii) the transition temperature should be tunable to allow for adapting the sensor according to varying legal temperature thresholds for temperature-controlled supply chains; and (iii) moreover, if the MSMA has once switched its state, it should not transform back to the initial state for all possibly occurring temperatures during operation, therefore a large thermal hysteresis is required. Hysteresis is an unwanted effect for magnetic shape memory for the application of magnetic refrigeration. In our application on the other hand, we take advantage of this distinct feature and utilize it for the performance of the proposed temperature indicator.

To investigate the tunability of the transition temperatures, a series of $Ni_{43}Mn_{46-x}Sn_{11}Co_x$ (x = 4, 4.5, 5.5, 6) alloys was prepared by arc melting. The precursor ingots were induction melted in a quartz tube and then ejected with 100 mbar pressurised argon onto a copper wheel rotating at a surface velocity of 30 m/s. The varying cobalt percentage was expected to yield different transition temperatures. To adjust the width of the thermal hysteresis and the sharpness of the transition, the melt-spun flakes were annealed at 1 173 K for 2 h. The thermal hysteresis of the magnetization was measured in a Physical Property Measurement System (PPMS) with a VSM at 50 Oe for as-spun and annealed flakes.

The annealed $Ni_{43}Mn_{40.5}Sn_{11}Co_{5.5}$ was then used to build a magnetoelastic resonance sensor: The sensor design is based on Sensormatic's EAS hard tag. The resonator comprises two adjacent magnetostrictive amorphous ribbons (38 mm × 12.5 mm × approximately 30 μm). The switch was made from 379 mg of the $Ni_{43}Mn_{40.5}Sn_{11}Co_{5.5}$ flakes, with a typical width of 2.5 mm to 3 mm and a typical length of 5 mm to 20 mm. They were distributed on an area of 46 mm × 13.5 mm with their long axis parallel to the sensors long axis and directly attached to the bias magnet. The original EAS tag uses a single bias magnet (43 mm × 13 mm × 1.1 mm). To compensate for the weakening of the effective bias field on the resonator by the switch, a second bias magnet of the same kind was attached, thus, maintaining an optimal operating point. The readout device was positioned in a free distance of 8 cm to the sensor. It

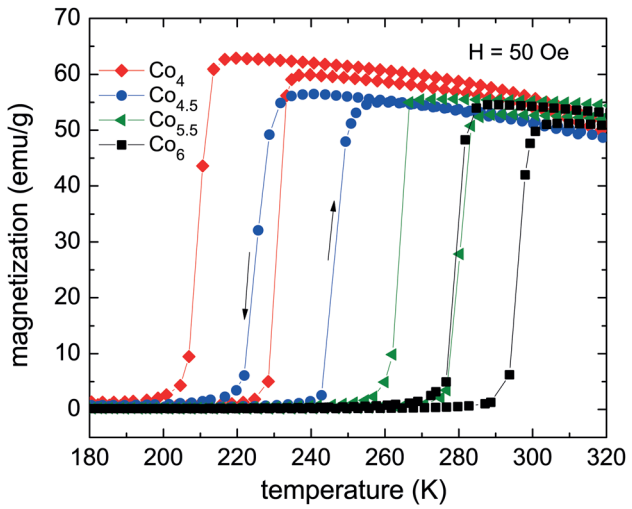

FIG. 3. Thermal hysteresis for melt-spun annealed flakes samples of $Ni_{43}Mn_{46-x}Sn_{11}Co_x$ (x = 4, 4.5, 5.5, 6).

comprises an excitation coil, which generates a magnetic AC field pulse to excite the resonator's vibrations. The frequency of the AC pulse is approximately 58 kHz, which is very close to the sensors resonant frequency. The readout device also comprises a pickup coil to measure the stray field of the resonator, which is freely vibrating after the AC pulse. The resonant frequency is determined from the frequency of the peak maximum in the fast Fourier transform of the measured signal. The sensor was placed in a vessel with controllable air temperature. The resonant frequency of the sensor was measured every second while the temperature was slowly varied in the range of the two transition temperatures.

The temperature dependence of the magnetization of the annealed $Ni_{43}Mn_{46-x}Sn_{11}Co_x$ samples is plotted in Figure 3 for varying Co contents. One can see that the martensite to austenite transition temperature could be tuned in a range of 230 K (4% Co) to 295 K (6% Co). Figure 4 shows the transition width and the width of the thermal hysteresis. Compared to the previously reported thermal hysteresis of 10 K for the bulk, the presented annealed flakes show a large hysteresis of about 20 K and a narrow transition width of 5–7 K. The flakes before annealing have an even larger thermal hysteresis, but the transition is less sharp, which is attributed to an inhomogeneous composition.

For many applications, a hysteresis of 20 K is sufficiently unforgeable: The information about transgression of upper limits can only be erased by cooling down by 20 K, which is often simply not possible with the available cooling units. An absolute forgery-proof sensor can be obtained by combining two of the proposed temperature indicators, where one monitors an upper temperature threshold and the other a lower one. Then neither of the indicators can be reset without tripping the other one.

The temperature sweep which has been performed on the described sensor with the $Ni_{43}Mn_{40.5}Sn_{11}Co_{5.5}$ switch and the associated variations in the resonant frequency are plotted in Figure 5. The slope of the first temperature rise is 1.75 K/min, all other slopes are 0.875 K/min.

The thermal hysteresis of the sensor signal during this temperature sweep can be seen in Figure 6 where the resonant frequency is plotted as function of the surrounding air temperature. The effect of the MSMA's phase transitions on the resonator's resonant frequency is distinct. On the rising branch, the resonant frequency jumps from 57 420 Hz to 57 700 Hz between 279 K and 290 K. On the downward branch, the jump occurs between 274 K and 264 K from 57 715 Hz to 57 430 Hz. The width of the thermal hysteresis is 16 K. Within this temperature range, a transgression of one of both transition temperatures is stored in the state of the switch. The plot shows that the height of the frequency leap is significant and can be used to clearly identify temperature transgressions. Due to the sensor's thermal inertia, the actual temperature inside the sensor needs some time to adapt to the surrounding temperature. Therefore, the branch measured at a faster temperature rise of 1.75 K/min is retarded by 1.6 K regarding the surrounding temperature compared to the branches at 0.875 K/min. This feature of thermal inertia can be controlled by the amount of switch material

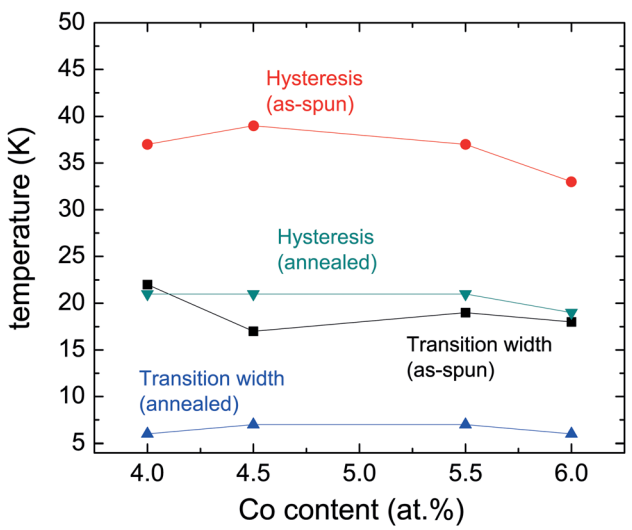

FIG. 4. Influence of chemical composition and annealing on transition width and thermal hysteresis for melt-spun flakes samples of $Ni_{43}Mn_{46-x}Sn_{11}Co_x$ (x = 4, 4.5, 5.5, 6).

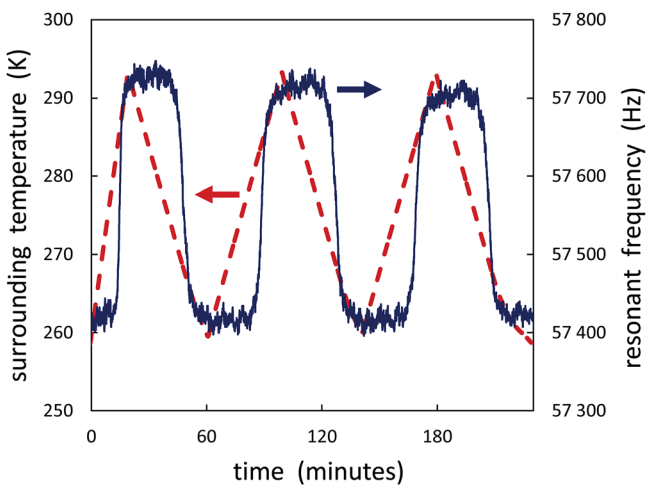

FIG. 5. Resonant frequency (continuous line) and surrounding temperature (dashed line) over time. The first temperature rise is at 1.75 K/min, all other slopes at 0.875 K/min. The frequency is represented by its moving average over ten samples.

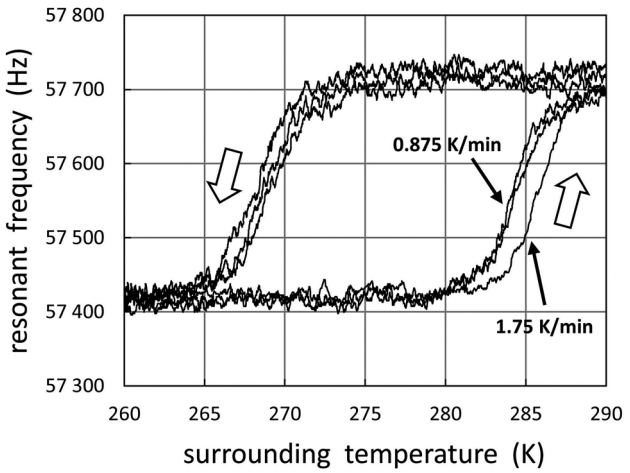

FIG. 6. Resonant frequency of a sensor containing 379 mg of annealed $Ni_{43}Mn_{40.5}Sn_{11}Co_{5.5}$ plotted against the surrounding temperature (moving average over ten samples).

and the sensor's isolation properties to match varying demands to the time-temperature-behaviour of temperature indicators for cold chain monitoring.

In summary, we presented an inexpensive Ni-Mn-Sn-Co switch material with sharp metamagnetic transitions with accompanying large hysteresis, which makes it suitable as a switch in a magnetoelastic resonance temperature indicator. Due to the precise tunability, the transition temperature can be adjusted according to the legal temperature threshold for a large range of products. Especially, dry ice transports at 217 K, frozen food at 254 K, and all kind of chilled goods below room temperature are covered by the demonstrated range of transition temperatures. The MSMA switch was integrated in a magnetoelastic resonance sensor. The state of the switch could be read out remotely by a readout device, which allows for detecting transgressions of the according transition temperatures. This makes the sensor an operational wireless temperature indicator, which needs no energy supply. All components of the sensor have very low material costs in the range of a few cents. Prices of competing wireless products such as active Radio-frequency identification (RFID) temperature loggers are in the range of 10 to 50 euros. As the proposed temperature indicators are based on the well developed acousto-magnetic EAS technology, we expect that they can be read out from a distance of up to 1.5 meters. For applications where strong physical shocks can occur, it should be considered that also mechanical stresses can induce a phase transition of the MSMA in the vicinity of the transition temperatures. The optimization of mass and geometry and the reproducible preparation of the MSMA switch as well as the long time stability of the switch under dynamic thermal load will be done in future work.

The authors would like to thank the WWTF project MA09-029, the FWF SFB ViCoM project F4112-N13, and the DFG (SPP 1239) for the financial support and Giselher Herzer and Roland Groessinger for the helpful discussions.

[1]G. Herzer, J. Magn. Magn. Mater. **254**, 598 (2003).
[2]C. A. Grimes, C. S. Mungle, K. Zeng, M. K. Jain, W. R. Dreschel, M. Paulose, and K. G. Ong, Sensors **2**, 294 (2002).
[3]C. A. Grimes, S. C. Roy, S. Rani, and Q. Cai, Sensors **11**, 2809 (2011).
[4]S. R. Green and Y. B. Gianchandani, J. Micromech. Microeng. **20**, 075040 (2010).
[5]T. Huber, B. Bergmair, C. Vogler, F. Bruckner, G. Hrkac, and D. Suess, Appl. Phys. Lett. **101**, 014102 (2012).
[6]H. A. Davies and M. R. J. Gibbs, in *Handbook of Magnetism and Advanced Magnetic Materials*, edited by H. Kronmüller and P. Stuart (Wiley, 2007).
[7]C. Liang, S. Morshed, and B. C. Prorok, Appl. Phys. Lett. **90**, 221912 (2007).
[8]J. D. Livingston, Phys. Status Solidi A **70**, 591 (1982).
[9]G. Herzer, Z. Metallkd. **93**, 978 (2002).
[10]G. Herzer, Mater. Sci. Eng., A **226-228**, 631 (1997).
[11]D. Suess and R. Groessinger, European patent 2280262 (2 February 2011).
[12]M. Nakamura, S. Yoshizawa, N. Kutsuzawa, S. Kambe, and O. Ishii, Phys. Status Solidi A **204**, 4137 (2007).
[13]R. Kainuma, Y. Imano, W. Ito, Y. Sutou, H. Morito, S. Okamoto, O. Kitakami, K. Oikawa, A. Fujita, T. Kanomata, and K. Ishida, Nature (London) **439**, 957 (2006).
[14]J. Liu, S. Aksoy, N. Scheerbaum, M. Acet, and O. Gutfleisch, Appl. Phys. Lett. **95**, 232515 (2009).
[15]L. Ma, H. W. Zhang, S. Y. Yu, Z. Y. Zhu, J. L. Chen, G. H. Wu, H. Y. Liu, J. P. Qu, and Y. X. Li, Appl. Phys. Lett. **92**, 032509 (2008).
[16]J. Liu, T. G. Woodcock, N. Scheerbaum, and O. Gutfleisch, Acta Mater. **57**, 4911 (2009).
[17]J. Liu, N. Scheerbaum, J. Lyubina, and O. Gutfleisch, Appl. Phys. Lett. **93**, 102512 (2008).
[18]T. Krenke, E. Duman, M. Acet, E. F. Wassermann, X. Moya, L. Maosa, and A. Planes, Nature Mater. **4**, 450 (2005).
[19]A. Planes, L. Maosa, and M. Acet, J. Phys. Condens. Matter **21**, 233201 (2009).
[20]J. Liu, T. Gottschall, K. P. Skokov, J. D. Moore, and O. Gutfleisch, Nature Mater. **11**, 620 (2012).
[21]Z. Han, D. Wang, B. Qian, J. Feng, X. Jiang, and Y. Du, Jpn. J. Appl. Phys., Part 1 **49**, 010211 (2010).